CHAPTER 4

COMPUTATIONAL FLUID DYNAMICS ANALYSIS OF A SHELL-AND-DOUBLE CONCENTRIC TUBE HEAT EXCHANGER

S.M. Shahril[1], Kahar Oman[2], M.K.R Hashim[1], A.M.N. Bariah[3], Ummikalsom Abidin[2], Nofrizalidris Darlis[4]

[1]Faculty of Mechanical Engineering Technology, University Malaysia Perlis (UniMAP), Pauh Putra, 02600 Arau, Perlis, Malaysia.

[2]Faculty of Mechanical Engineering, Universiti Teknologi Malaysia, 81310 Johor Bahru, Johor, Malaysia

[3]Faculty of Electrical Engineering Technology, Universiti Malaysia Perlis(UniMAP), Pauh Putra Campus, 02600 Arau, Perlis, Malaysia

[4]Centre of Automotive & Powertrain Technology, Faculty of Engineering Technology, University Tun Hussein Onn Malaysia, Edu Hub Pagoh, 84600, Muar, Johor, Malaysia

ABSTRACT

Shell-and-tube heat exchangers (STHEX) have been used for several decades. Conventionally, to increase the thermos-hydraulic performance of classical heat exchangers, the overall length of tubes has to be increased. This contributes to major disadvantages in terms of classical heat exchangers' design, particularly considering the economic aspect. In this study, the thermo-hydraulic performance analysis of a shell-and-double concentric tube heat exchanger (SDCTHEX) is carried out using commercially available Computational Fluid Dynamics (CFD) software ANSYS FLUENT. The results show that the average percentage increase in overall heat transfer rate per overall pressure drop of SDCTHEX, with inner tube diameter equal to 8/12 mm/mm, is nearly 343% higher than that of STHEX, while the total friction power expenditure of SDCTHEX is reduced by around 85.5% as compared to that of STHEX. Also, the overall heat transfer rate per overall pressure drop of SDCTHEX is sensitive to inner tube diameter. It is found that U=DP for the mass flow rate of 22.5 kg/s is maximum and found to be about 400% higher at inner tube diameter of 12/16 mm/mm with respect to the STHEX. The results of simulation present that, the SDCTHEX has a higher heat transfer performance while maintaining a lower pressure drop.

Keywords: Shell-and-tube heat exchangers, CFD, thermo-hydraulic

4.1 INTRODUCTION

Shell-and-tube heat exchangers (STHEX) are widely regarded as the cornerstone of industrial heat exchange systems, surpassing other types of heat exchangers in both application and reliability (Marzouk, et. al, 2022). Their predominant use across various sectors is attributed to well-established design and manufacturing protocols, decades of proven operational performance, and the availability of comprehensive codes and standards that govern their design and fabrication. These heat exchangers are employed extensively across a broad range of industrial processes, including chemical production, power generation, food processing, distillation, cryogenics, and waste heat recovery. Despite their widespread adoption, shell-and-tube heat exchangers present several operational limitations. Common issues include significant fouling in stagnant or dead flow zones, vibration-induced damage within the tube bundle, and relatively high energy consumption (Mehrjardi, et. al, 2024). As a result, these challenges have attracted considerable academic and industrial interest aimed at improving the performance and reliability of STHEX configurations.

While analytical methods are useful for identifying potential design inefficiencies, they are limited in their ability to localise specific problem areas within the heat exchanger. In this context, CFD offers a powerful alternative, enabling detailed visualisation of the flow and temperature fields, particularly on the shell side. This insight facilitates a more precise evaluation of performance-limiting features and informs targeted design modifications to enhance overall efficiency (Mohammadzadeh, et. al, 2024). However, conducting CFD analyses on a full-scale STHEX model using commercial software demands significant computational resources. It is well-established that full-model simulations yield the most accurate predictions of thermo-hydraulic performance compared to simplified or segmented models. Accordingly, the present study aims to investigate the heat transfer and flow characteristics of a Shell-and-Double Concentric Tube Heat Exchanger (SDCTHEX) proposed by Bougriou and Baadache [4] and compare its performance against the conventional Shell-and-Tube Heat Exchanger (STHEX). The study employs CFD simulations using ANSYS FLUENT 14, with the geometric and operational parameters of the SDCTHEX and STHEX closely based on the configurations reported in (Bougriou, 2010).

4.2 METHODOLOGY

4.2.1 Physical Model

The geometric configurations of the STHEX and the SDCTHEX are illustrated in Fig. 4.1 and
Fig. **4.2**, respectively. Both models share identical shell dimensions, with an internal diameter of 337 mm, and are designed to accommodate 55 tubes arranged in a staggered pattern. The effective heat transfer length for both the shell and tubes is 1270 mm. In the STHEX configuration, the tubes have an external diameter (D_2) of 24 mm and an internal diameter (D_1) of 20 mm. The tubes and baffles are fabricated from AISI 1042-annealed steel, which possesses a density of 7840 kg/m^3, a thermal conductivity of 50 W/m·K, and a specific heat capacity of 460 J/kg·K. Baffle spacing is uniformly set at 100 mm, with each baffle having a thickness of 5 mm. Both heat exchanger models operate with a single shell pass and a single tube pass. The SDCTHEX model is further distinguished by the incorporation of inner concentric tubes within each primary tube. These inner tubes have an internal diameter (d_1) of 8 mm and an external diameter (d_2) of 12 mm, enabling additional heat transfer surface area and fluid flow channels. The thermophysical properties of the working fluids, unused engine oil as the hot fluid and water as the cold fluid, are defined as temperature-dependent piecewise linear functions and implemented in the simulation using ANSYS FLUENT 14.0.

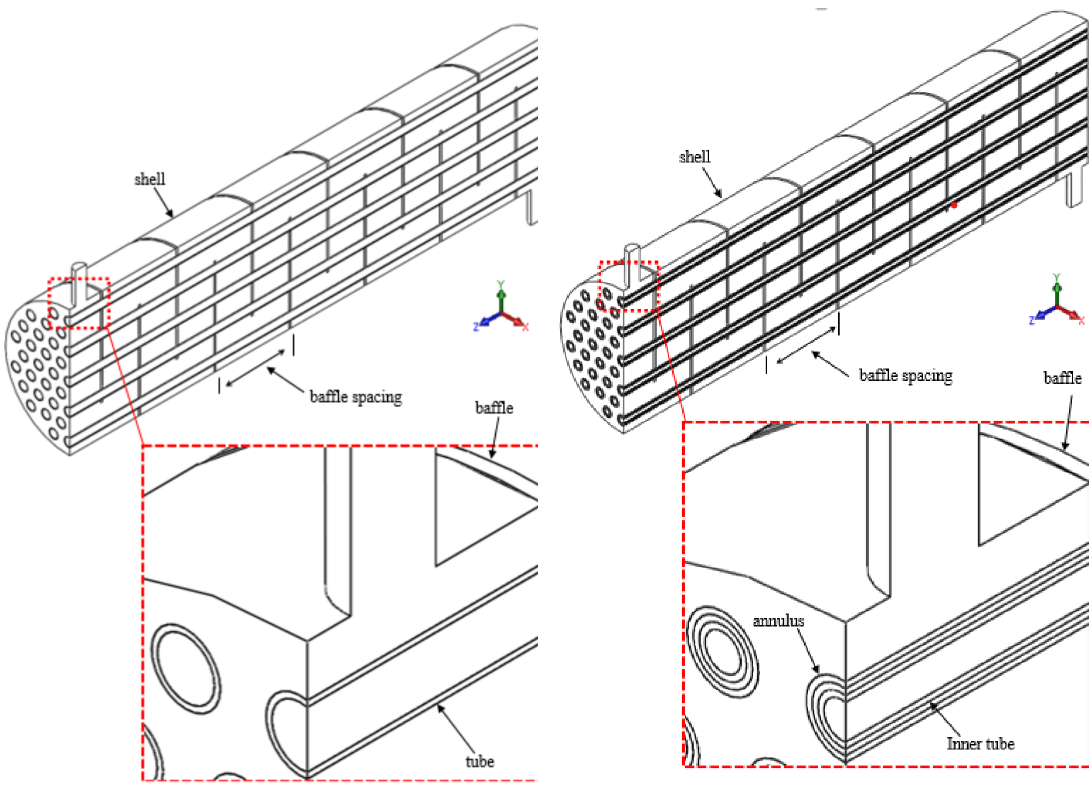

(a) STHEX (b) SDCTHEX

Fig. 4.1: Isometric view of both geometries of heat exchangers

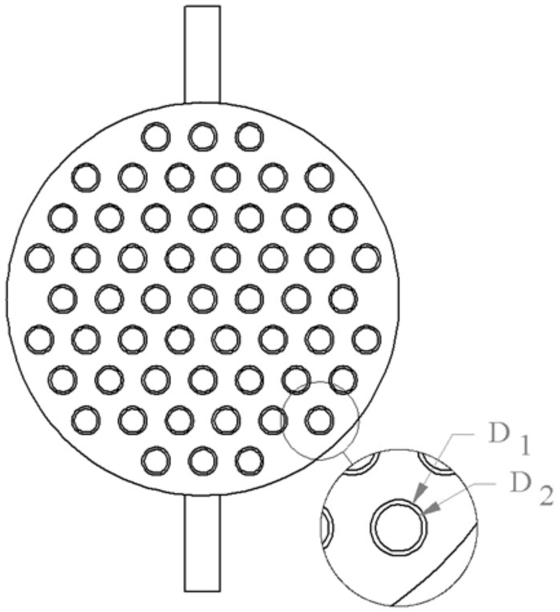

(a) STHEX

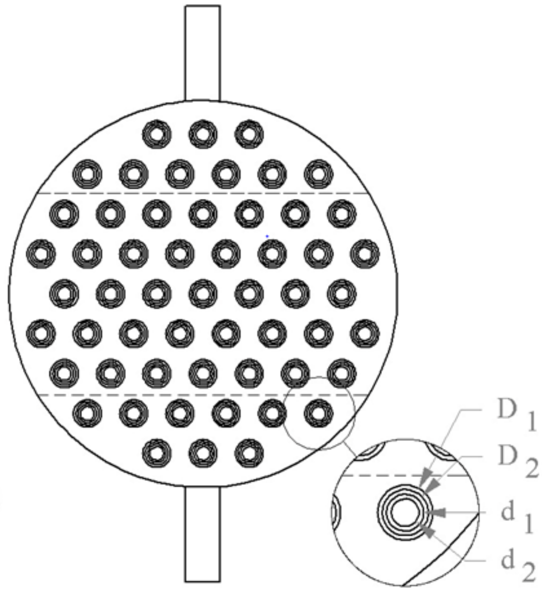

(b) SDCTHEX

Fig. 4.2: Tube arrangement inside heat exchangers

4.2.2 Governing Equations

The main focus of the present study is to predict the overall thermo-hydraulic performance for both models of heat exchangers under the assumptions of steady-state conditions, flow being turbulent, fully developed and incompressible. For this, the realizable *k-ε* turbulence model is adopted because it can accurately predict near-wall flows and flows with high streamline curvature, vortices, and rotation (Ozden, 2010).

The governing equations for continuity, momentum, energy conservation, kinetic energy, *k,* and turbulent energy dissipation, *ε* can be written as follows:

Continuity equation:

$$\frac{\partial u_i}{\partial x_i} = 0 \tag{1}$$

Momentum equation:

$$\frac{\partial u_i u_j}{\partial x_i} = -\frac{1}{\rho}\frac{\partial \rho}{\partial x_i} + \frac{\partial}{\partial x_j}\left(\left(v + v_t\right)\left(\frac{\partial u_j}{\partial u_i} + \frac{\partial u_i}{\partial x_j}\right)\right) \tag{2}$$

Energy equation:

$$\frac{\partial u_i T}{\partial x_i} = \frac{\partial}{\partial x_i}\left(\left(\frac{v}{\Pr} + \frac{v_t}{\Pr_t}\right)\frac{\partial T}{\partial x_i}\right) \tag{3}$$

Turbulent kinetic energy, *k* equation:

$$\frac{\partial u_i k}{\partial x_i} = \frac{\partial}{\partial x_i}\left(\left(v + \frac{v_t}{\sigma_k}\right)\frac{\partial k}{\partial x_i}\right) + \Gamma - \varepsilon \tag{4}$$

Turbulent energy dissipation, *Ɛ* equation:

$$\frac{\partial u_i \varepsilon}{\partial x_i} = \frac{\partial}{\partial x_i}\left(\left(v + \frac{v_t}{\sigma_\varepsilon}\right)\frac{\partial \varepsilon}{\partial x_i}\right) - C_2 \frac{\varepsilon^2}{k + \sqrt{v\varepsilon}} \tag{5}$$

where

$$\Gamma = -\bar{u}_i \bar{u}_j \frac{\partial u_i}{\partial x_j} = v_t \left(\frac{\partial u_i}{\partial x_j} + \frac{\partial u_j}{\partial x_i}\right)\frac{\partial u_i}{\partial u_i} \tag{6}$$

$$v_t = C_\mu \frac{k^2}{\varepsilon} \tag{7}$$

The empirical constant for the realizable *k*-ε turbulence model is assigned as follows: $C_2 = 1.9$, $\sigma_k = 1.0$, $\sigma_\varepsilon = 1.2$. In other high Reynolds number turbulence models, c_μ is a constant. However, to achieve the realizable effects, c_μ becomes a function of the rotation rates (angular velocity) and strain (turbulence fields). It is calculated from

$$C_\mu = \frac{1}{A_0 + A_s \dfrac{kU^*}{\varepsilon}} \tag{8}$$

where $A_0 = 4.04$ constant along the simulation. Other parameters in Eq. (8) are as follows:

$$U^* = \sqrt{S_{ij} S_{ij} + \tilde{\Omega}_{ij} \tilde{\Omega}_{ij}} \tag{9}$$

$$A_s = \sqrt{6}\cos\phi$$
(10)

where $\widetilde{\Omega}_{ij} = \Omega_{ij}\,(\Omega_{ij} = \overline{\Omega}_{ij} - \varepsilon_{ijk}\omega_k)$ and $\phi = \frac{1}{3}\cos^{-1}\left(\sqrt{6}W\right)$. Term W and $\widetilde{S}$ are given by

$$W = \frac{S_{ij}S_{jk}S_{ki}}{\widetilde{S}^3} \quad (11)$$

$$\widetilde{S} = \sqrt{S_{ij}S_{ij}} \quad (12)$$

where

$$S_{ij} = \frac{1}{2}\left(\frac{\partial u_j}{\partial x_i} + \frac{\partial u_i}{\partial x_j}\right) \quad (13)$$

Proper near-wall treatment is crucial for turbulent flow and heat transfer because the non-dimensional distance from the wall to the first mesh node (y*) is important. Wall functions often face issues with inconsistency in the position of the points nearest to the wall and sensitivity to near-wall meshing. To address this, ANSYS FLUENT 14.0 uses a scalable wall function for improved mesh refinement at the wall, which is consistent regardless of the Reynolds number. This scalable wall function was used in all simulations to limit y* to a maximum of 11.225. For coarse grids where y* > 11.225, the results are the same as the standard wall function. It is recommended to use scalable wall functions with the k-ε turbulence model(Marzouk, et. al, 2024)[1].

4.2.3 Boundary Condition and the numerical method

The working fluids within the shell and tubes for STHEX are hot engine oil and cold water, respectively. In SDCTHEX, the working fluid for the shell and inner tube side is hot engine oil while the working fluid for the annulus formed between the two concentric tubes is cold water. Therefore, the mass flow rate of the engine oil circulating in the shell for STHEX is equally divided between the shell side and inner tube side of the SDCTHEX. The cooling water circulates counter-flow in the annular passage formed by the concentric tubes.

Tables 4.1 and 4.2 give the details of the boundary conditions imposed for simulating the two different heat exchangers for particular mass flow rates on the shell side, inner tube side, and annulus side. It is to be noted that the boundary conditions will change for different mass flow rates.

Table 4.1: Boundary Conditions for Shell-and-Tube Heat Exchanger

Item/Boundary zone	Boundary condition
Inlet nozzle wall, outlet nozzle walls, outside baffles wall, and shell wall	Heat flux is zero(adiabatic)
Inlet shell nozzle	Velocity inlet: flows normal to the inlet cross-sectional area (mass flow rate = 20 kg/s), and constant stream temperature is equal to 393 K, i.e. 120°C.
Inlet annulus	Velocity inlet: flow normal to the inlet cross-sectional area (mass flow rate = 10.14 kg/s) and constant stream temperature is equal to 293 K, i.e 20°C.
Inlet inner tube	Velocity inlet: flows normal to the inlet cross-sectional area (mass flow rate = 20 kg/s) and constant stream temperature is equal to 393 K, i.e. 120°C.
Outlet shell nozzle	Pressure outlet
Outlet annulus	Pressure outlet
Outlet inner tube	Pressure outlet
Tube wall and inside baffle wall	Conjugate heat transfer

Table 4.2. Boundary conditions for Shell-and-Double concentric Tube Heat Exchanger

Item/Boundary zone	Boundary condition
Inlet nozzle wall, outlet nozzle walls, outside baffles wall, and shell wall	Heat flux is zero(adiabatic)
Inlet shell nozzle	Velocity inlet flows normal to the inlet cross-sectional area (mass flow rate = 40 kg/s), and constant stream temperature is equal to 393 K, i.e. 120°C.
Inlet tube	Velocity inlet: flows normal to the inlet cross-sectional area (mass flow rate = 10.14 kg/s) and constant stream temperature is equal to 293 K, i.e. 20 °C
Outlet shell nozzle	Pressure outlet
Outlet tube	Pressure outlet

Item/Boundary zone	Boundary condition
Tube wall and inside baffle wall	Conjugate heat transfer

Zero-gauge pressure is assigned to the inlets and outlets of both heat exchanger models to measure the relative pressure drop. All wall surfaces use no-slip boundary conditions. The shell walls are adiabatic, while the tube walls, annulus walls, and baffle walls use coupled thermal boundaries. Leakage through baffle hole clearances is ignored. The second-order upwind scheme was applied for energy and momentum calculations, and the SIMPLE algorithm was used for pressure-velocity coupling as integrated in ANSYS FLUENT 14.0. The default under-relaxation factors are 0.3 for pressure, 0.7 for momentum, 0.8 for turbulent kinetic energy, and 0.7 for turbulent energy dissipation. Convergence is achieved when the normalised absolute residuals are below 10^{-6} for flow variables and 10^{-7} for energy variables. A parallel computation is performed on a server with eight Intel Xeon-core CPUs and 24 GB RAM each, taking about 15 hours per case to converge.

4.2.4 Data Reduction

4.2.4.1 Shell-and-Tube heat exchanger

Under the steady flow conditions, the energy balance of STHEX is given by:

$$\Phi = \Phi_s + \Phi_t \tag{14}$$

where,
$\Phi_s = m_s c_{ps}(T_{s,in} - T_{s,out})$ and $\Phi_t = m_t c_{pt}(T_{t,in} - T_{t,out})$. The superscripts "*in*" and "*out*" stand for the values at the inlet and outlet, respectively; the subscripts "*s*" and "*t*" refer to the values on the shell side and tube side, respectively. The average heat transfer rate, Φ_{av} between two fluids is determined as $\Phi_{av} = (\Phi_s + \Phi_t)/2$ to calculate the heat transfer coefficient on the tube side given by:

$$h_t = \frac{\Phi_{av}}{A_t(T_w - T_b)} \tag{15}$$

where A_t is the heat transfer area on the tube surface; T_w is the tube wall temperature; T_b is the bulk fluid temperature of the fluid inside the tubes. Since the current heat exchanger takes the counter current arrangement, the logarithmic mean temperature difference can be expressed as:

$$\Delta T_{m_{1,2}} = \frac{(T_{s,in} - T_{t,out}) - (T_{s,out} - T_{t,in})}{\ln \dfrac{(T_{s,in} - T_{t,out})}{(T_{s,out} - T_{t,in})}} \tag{16}$$

The overall heat transfer coefficient from the shell side to the tube side, based on the outside surfaces of the tubes, is calculated by the heat transfer equation:

$$U = \frac{\Phi_{av}}{N_t \pi D_1 L_t F \Delta T_m} \tag{17}$$

where L_t refers to the effective heat transfer length of tubes, D_1 refers to the outside tube diameter, and F is the correction factor for counter flow LMTD, respectively.

The shell side convection heat transfer coefficient is calculated by:

$$h_s = \frac{1}{\dfrac{1}{U} - \dfrac{1}{h_t}\dfrac{D_1}{D_2} - \dfrac{D_1}{2\lambda_t}\ln\dfrac{D_1}{D_2}} \tag{18}$$

where D_2 refers to the inside tube diameter, while the heat conductivity of the tube is expressed by λ_t, and U is the overall heat transfer coefficient obtained by Eq.(17).

4.2.4.1 Shell-and-Double Concentric Tube heat exchanger

For the same flow conditions, the energy balance for SDCTHEX is given by:

$$\Phi_a = \Phi_s + \Phi_i \tag{19}$$

where,

$$\Phi_a = m_a c_{pa}(T_{a,out} - T_{a,in});\ \Phi_s = m_s c_{ps}(T_{s,in} - T_{s,out});\Phi_i = m_i c_{pi}(T_{i,in} - T_{i,out})$$

where the subscript "*a*" refers to the annulus side. The average heat transfer rate, Φ_{av} is determined as : $\Phi_{av} = (\Phi_a + \Phi_{s,i})/2$ where $\Phi_{s,i} = (\Phi_s + \Phi_i)$.

Since the annulus flow is in the counter-current arrangement, the logarithmic mean temperature difference between the shell side and the annulus side can be expressed as:

$$\Delta T_{m_{1,2}} = \frac{\left(T_{s,in} - T_{a,out}\right) - \left(T_{s,out} - T_{a,in}\right)}{\ln \frac{\left(T_{s,in} - T_{a,out}\right)}{\left(T_{s,out} - T_{a,in}\right)}} \tag{20}$$

and the logarithmic mean temperature difference between the inner tube side and the annulus side can be expressed by:

$$\Delta T_{m_{2,3}} = \frac{\left(T_{i,in} - T_{a,out}\right) - \left(T_{i,out} - T_{a,in}\right)}{\ln \frac{\left(T_{i,in} - T_{a,out}\right)}{\left(T_{i,out} - T_{a,in}\right)}} \tag{21}$$

The heat transfer coefficient on the inner tube side is calculated using Eq. (15). The overall heat transfer coefficient from the annulus side to the inner tube side, based on the outside surfaces of the inner tubes, is calculated by the heat transfer equation:

$$U_{2,3} = \Phi_i / N_i \pi d_1 L_i \Delta T_{m\ 2,3} \tag{22}$$

The annulus side convection heat transfer coefficient is calculated by

$$h_a = \frac{1}{\frac{1}{U_{2,3}} - \frac{1}{h_t}\frac{d_1}{d_2} - \frac{d_1}{2\lambda_i}\ln\frac{d_1}{d_2}} \tag{23}$$

where d_1 and d_2 refer to the inner tube outside diameter and inner tube inside diameter, respectively.

The overall heat transfer coefficient from the shell side to the annulus side, based on the outside surface of the annulus, is calculated by the heat transfer equation:

$$U_{1,2} = \Phi_s / N_a \pi D_1 L_a F \Delta T_{m\ 1,2} \tag{24}$$

The shell side convection heat transfer coefficient is calculated by:

$$h_s = \frac{1}{\frac{1}{U_{1,2}} - \frac{1}{h_a}\frac{D_1}{D_2} - \frac{D_1}{2\lambda_a}\ln\frac{D_1}{D_2}} \tag{25}$$

where D_1 and D_2 refer to the annulus outside diameter and annulus inside diameter, respectively.

4.2.5 Grid System and Validation of the Numerical Models

The 3D geometry for the heat exchanger models was created using commercial CAD software and meshed with unstructured Tet/Hybrid grids in ICEM CFD ANSYS as shown in Fig. 4.3, which effectively manages complex geometries. The main parameter that defined the mesh size was the number of elements on the tube wall and annulus wall for STHEX and SDCTHEX, respectively. On these walls, the total numbers of mesh elements were controlled at a number of element divisions under sizing control on the tube wall and annulus wall for two parameters, namely length and diameter, as shown in Fig. 4.4.

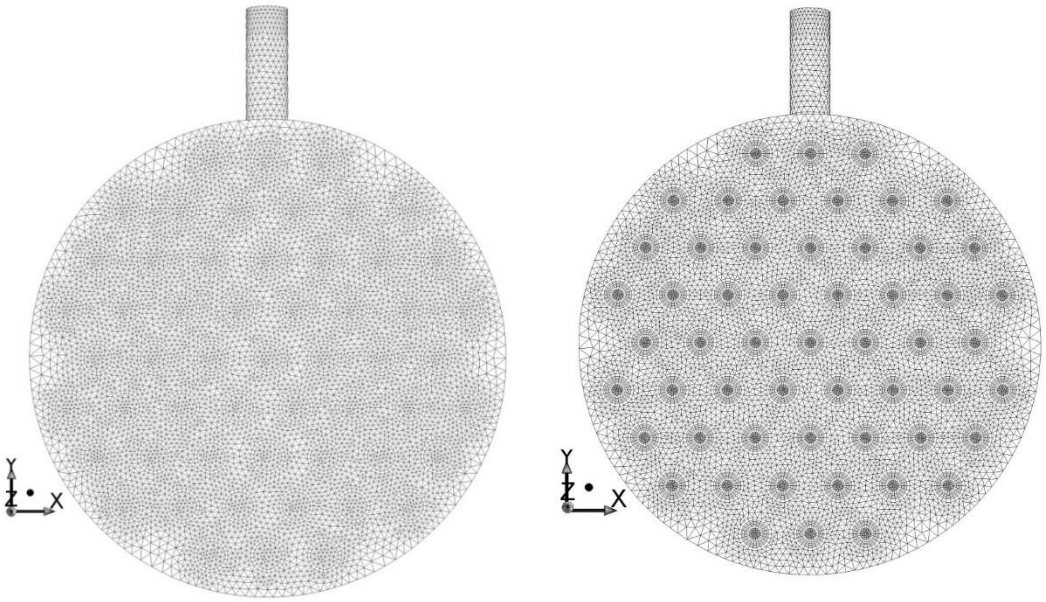

(b) Side view of the grid for STHEX (c) Side view of the grid for SDCTHEX

Fig. 4.3: Meshes of computational models

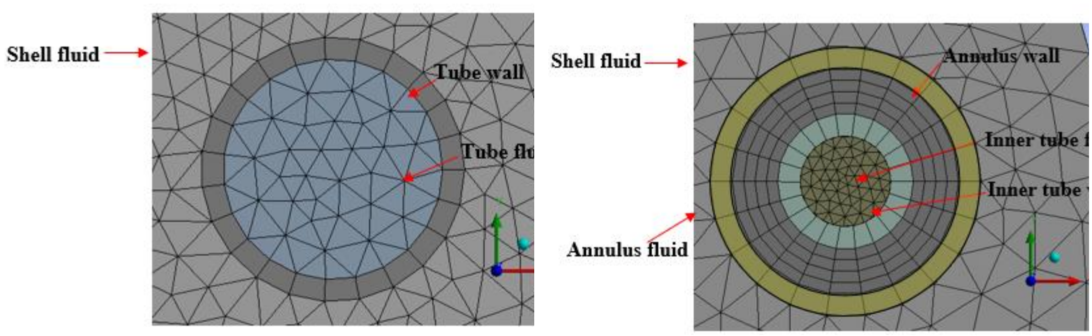

(a) (b)

Fig. 4.4: Mesh control for (a) SDCTHEX, and (b) STHEX

The total number of mesh elements, i.e. the mesh size, for the STHEX with 55 tubes when changing those two parameters were 4552601, 5360448, 6255624, 10582784, and 15178146. Meanwhile, the SDCTHEX for the same number of tubes were 4050419, 7303083, 10236633, 15583478, and 20896404. All five mesh models were used to perform calculations applying the CFD setup presented in Section 2.3. From the numerical simulation results, it is found that the relative deviation of the overall heat transfer rate (expressed in its average value) and overall pressure drop between the last two mesh systems is less than 1 % for both models. Therefore, all the results presented hereafter correspond to the last two mesh systems (element numbers shown in bold) for the models described earlier, considering both solution accuracy and computational time consumption.

To validate the models in terms of shell-side heat transfer coefficients and pressure drops, several empirical correlations including the Bell-Delaware method are adopted. The Bell-Delaware method is known for its accuracy in estimating these parameters for common shell-side geometries of STHEX. Fig. 4.5 and Fig. 4.6 compare the CFD simulation results with the Bell-Delaware method results for various shell-side mass flow rates. For STHEX, the average deviation between CFD and Bell-Delaware results is 8.4% for the shell-side heat transfer coefficient and 2.9% for the shell-side pressure drop. For SDCTHEX, the deviations are 9% and 2.6% respectively. These deviations are within acceptable ranges, confirming the reliability of the simulation results.

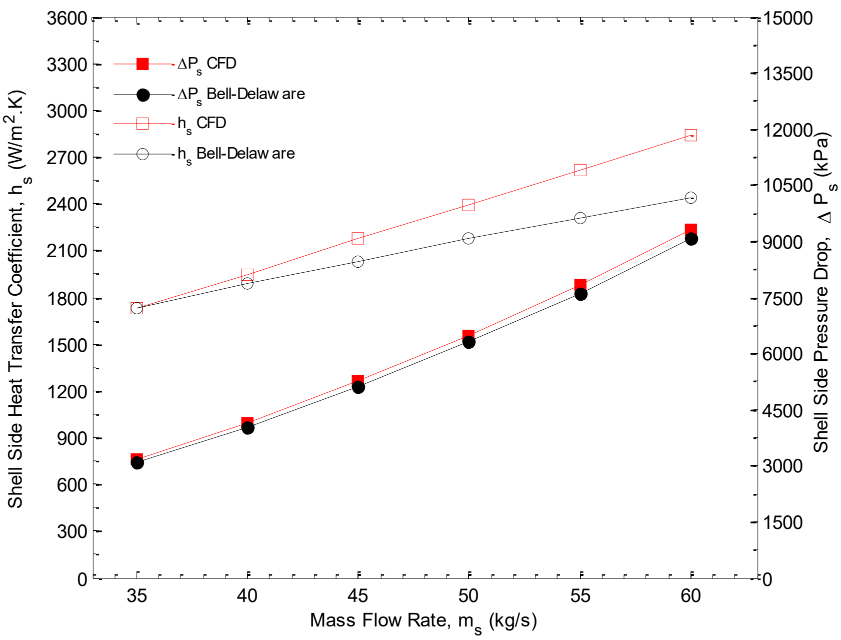

Fig. 4.5: Shell side heat transfer coefficient and pressure drop with different mass flow rates, m_s for STHEX.

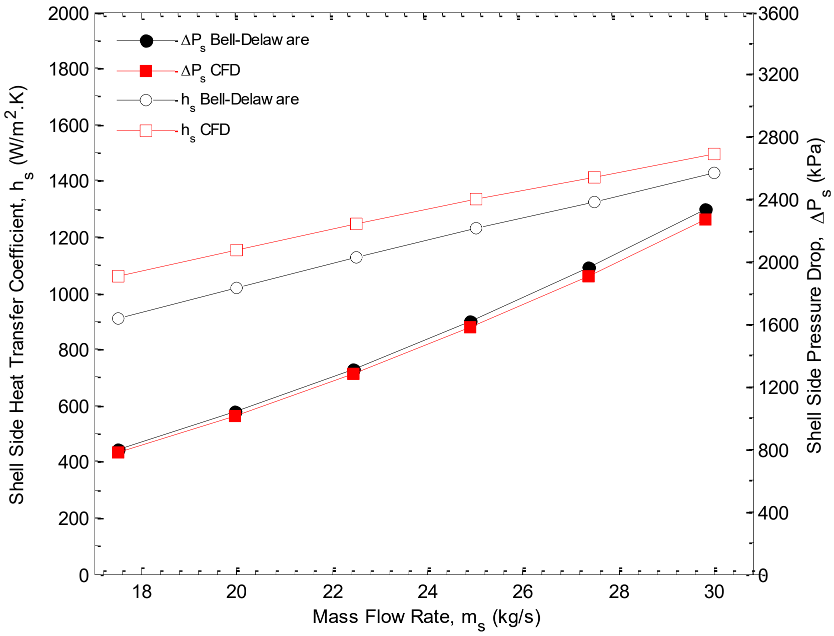

Fig. 4.6: Shell side heat transfer coefficient and pressure drop with different mass flow rates, m_s for SDCTHEX

The overall pressure drop ΔP is the sum of the pressure drop on the shell side, ΔP_s and that on the tube side, ΔP_t. Similarly, the overall heat transfer rate, Φ is the sum of the heat transfer rate on the shell side, Φ_s, and that on the tube side for STHEX. An additional corresponding term for the annulus side is to be considered for the SDCTHEX. The Bell-Delaware method does not predict ΔP_t, Φ_t, ΔP_a, or Φ_a. To find them, one has to resort to additional empirical correlations such as that given by Gneilinski. Results obtained by the additional correlation are termed Bell-Delaware + Gneilinski results as shown in the legends of Fig. 4.7 and Fig. 4.8, and others as well.

$$Nu = \frac{(f/2)(\mathrm{Re}_t - 1000)\mathrm{Pr}}{1 + 12.7\sqrt{(f/2)^{1/2}}\left(\mathrm{Pr}^{2/3} - 1\right)} \tag{26}$$

where *Re*, *Pr* refer to the Reynolds number and Prandtl number, respectively: *f* is the friction factor proposed by *Haaland* used as follows :

$$\frac{1}{\sqrt{f}} \cong -1.8\log\left[\frac{6.9}{\mathrm{Re}} + \left(\frac{\varepsilon/D}{3.7}\right)^{1.11}\right] \tag{27}$$

For flow in tube side, annulus side and inner tube side, the heat transfer coefficient h_t, h_a, and h_i are defined as

$$h_t = \frac{Nu_t \lambda_t}{d_h},\ h_a = \frac{Nu_a \lambda_a}{d_h},\ \text{and}\ h_i = \frac{Nu_i \lambda_i}{d_h}. \tag{28}$$

For fully-developed fluid flow inside a tube or annulus (neglecting the entrance effect), the pressure drop ΔP can be calculated as:

$$\Delta P = f \frac{1}{2} \rho v^2 \frac{L}{D_h} \tag{29}$$

where f is the friction factor calculated from Eq. (27), L is effective length, D_h is hydraulic diameter, V is the average or mean working fluid velocity and ρ is the fluid density. Note that here, the physical properties of the fluid are assumed constant. The value of surface roughness, ε for steel is taken as 0.000045 m to be used in Eq. (27).

The overall heat transfer rate and overall pressure drop obtained from simulation and also from the Bell-Delaware + Gnielinski correlations for STHEX and SDCTHEX, have been presented in Fig. 4.7 and Fig. 4.8. It can be observed from Fig. 4.7 that the average deviation between the numerical results and those from the Bell-Delaware + Gnielinski correlations is around 4.1% and 2.8% for the overall heat transfer rate and overall pressure drop, respectively, for STHEX. From Fig. 4.8, these deviations are found to be 4.7% and 0.8% for the SDCTHEX. It may be pointed out again that these deviations are within the acceptable range. All the above exercises suggest that the simulation results are well-validated. It can, therefore, be concluded that thermo-hydraulic performances, especially for the SDCTHEX model could be predicted satisfactorily by the present numerical model.

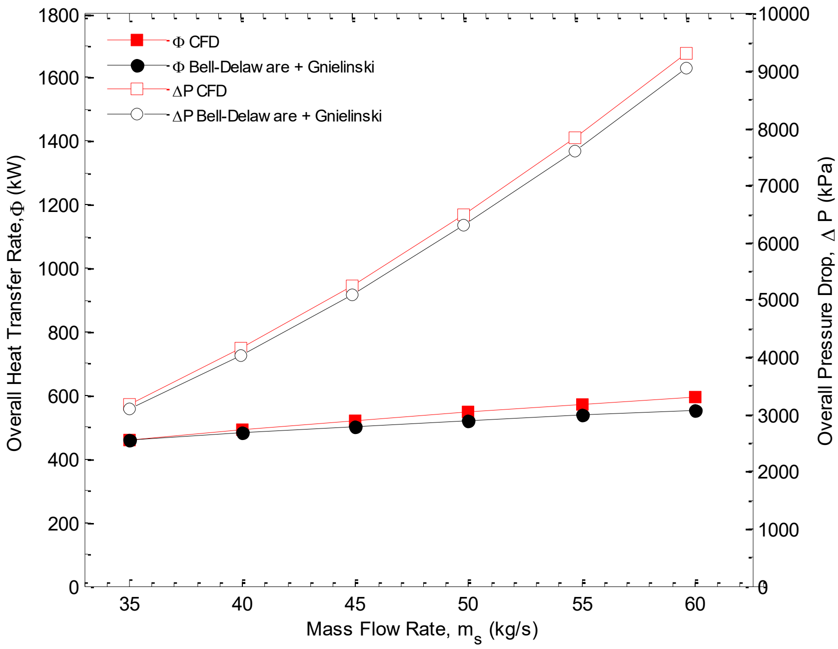

Fig. 4.7: Shell side heat transfer coefficient and pressure drop with different mass flow rates, m_s for STHEX

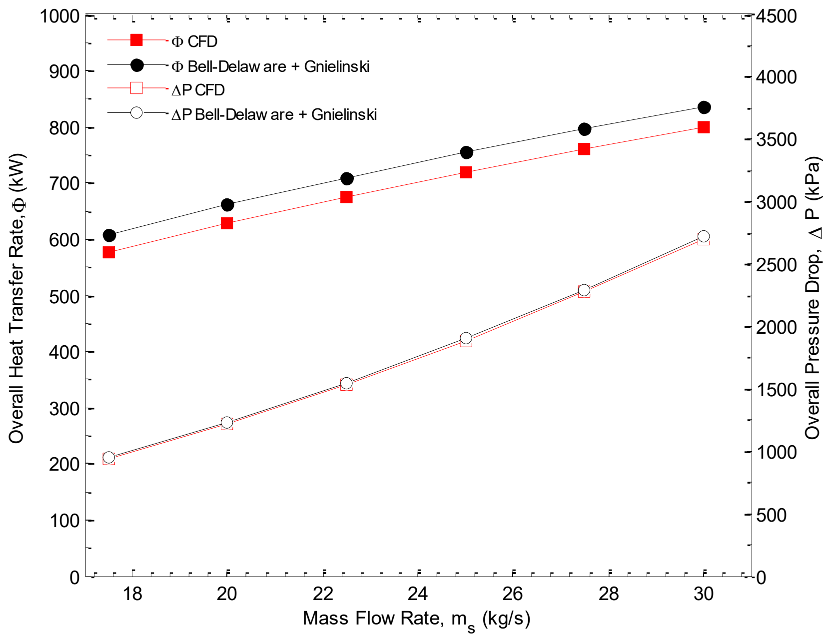

Fig. 4.8: Shell side heat transfer coefficient and pressure drop with different mass flow rates, m_s for SDCTHEX

4.3 RESULTS AND DISCUSSION

To evaluate and compare the performance of the two heat exchanger configurations, several key performance parameters are analyzed. As illustrated in Fig. 4.9, the overall heat transfer coefficients, namely $U_{1,2}$ (between the shell side and the annulus side), $U_{2,3}$ (between the annulus side and the inner tube side), and

U (for the conventional STHEX), increase with increasing mass flow rate of the hot fluid (m_s). This trend is attributed to enhanced convective heat transfer at higher flow rates. Among the coefficients, $U_{2,3}$ demonstrates the highest values, suggesting that the heat transfer within the inner tube of the SDCTHEX is more effective. Consequently, the SDCTHEX outperforms STHEX in terms of overall heat transfer efficiency, highlighting its potential as a superior alternative for thermal performance enhancement.

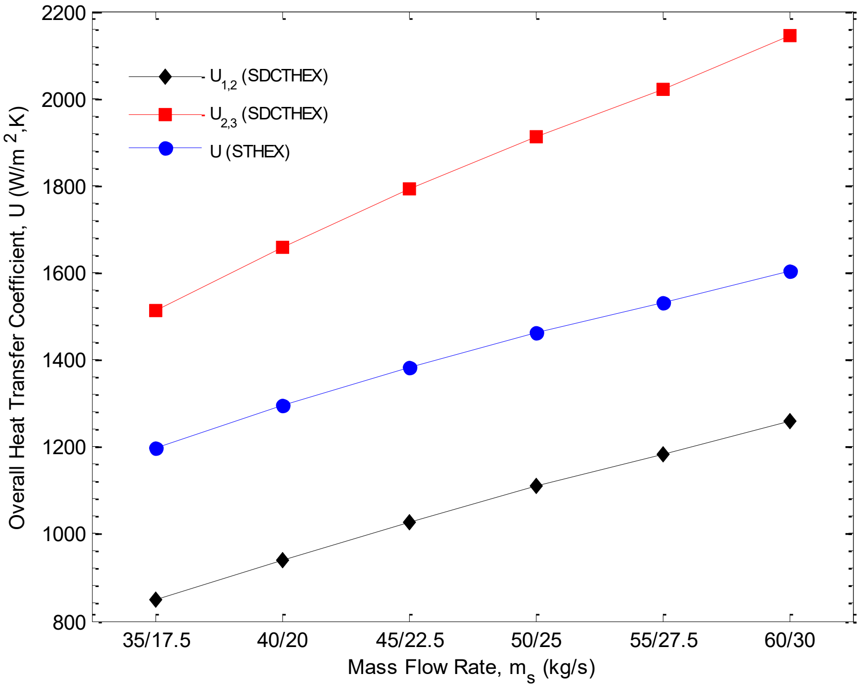

Fig. 4.9. Overall heat transfer coefficient with different mass flow rates, m_s for STHEX and SDCTHEX

Fig. 4.10 illustrates the variation in overall heat transfer rate and pressure drop as a function of the hot fluid mass flow rate for both heat exchanger configurations. As expected, both the heat transfer rate and pressure drop increase with rising mass flow rate due to intensified convective activity and higher flow resistance. The SDCTHEX demonstrates superior thermal performance, with a heat transfer rate that is 25.3% higher than that of the STHEX at a mass flow rate of 17.5 kg/s, and this advantage increases to 34.6% at 30.0 kg/s. This improvement is attributed to the presence of the additional inner tube in the SDCTHEX, which provides an expanded heat transfer surface area and enhanced thermal interaction.

In addition to improved thermal performance, the SDCTHEX exhibits significantly lower overall pressure drops across all tested flow rates. This reduction is primarily due to lower flow velocities within the shell side and the inner tube, resulting in decreased flow resistance. At the lowest tested mass flow rate, the pressure drop in the SDCTHEX is approximately 70.4% lower than that of the

STHEX; this difference increases marginally to 71.1% at the highest flow rate. Since pressure drop is directly related to the pumping power requirement, a lower pressure drop translates to reduced operational costs. Therefore, the SDCTHEX offers two critical advantages over the conventional STHEX: enhanced heat transfer rates and significantly reduced pressure losses, making it a more energy-efficient and cost-effective option for industrial heat exchange applications.

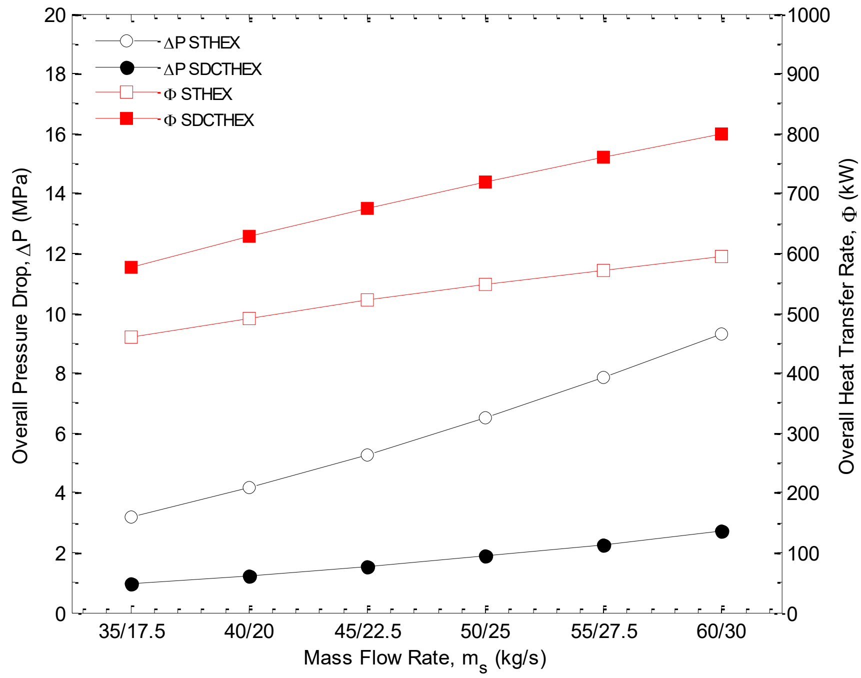

Fig. 4.10: Shell side heat transfer coefficient and pressure drop against mass flow rate m_s for STHEX and SDCTHEX

4.4 CONCLUSION

In this study, ANSYS FLUENT 14.0 is used to predict the thermo-hydraulic performance of a shell-and-double concentric tube heat exchanger (SDCTHEX) at different hot fluid mass flow rates and compare it with a classical shell-and-tube heat exchanger (STHEX). The following conclusions are drawn from the analysis:

1. The CFD results for the entire heat exchanger, including tubes, baffles, and different fluids on the shell, annulus, and tube sides, are successfully validated against the Bell-Delaware method and other empirical correlations.
2. The overall heat transfer rate and pressure drop increase with higher hot fluid mass flow rates for both heat exchangers. However, the increase in heat transfer rate is greater for the SDCTHEX compared to the STHEX, while the pressure drop is consistently lower for the SDCTHEX.

3. Therefore, the SDCTHEX is a promising alternative for industrial heat transfer applications compared to the classical STHEX.

4.5 ACKNOWLEDGEMENT

The authors thank to the Universiti Malaysia Perlis (UniMAP) and Faculty of Mechanical Engineering & Technology at UniMAP for its practical support.

4.6 REFERENCE

Marzouk, S. A., Al-Sood, M. M. A., El-Fakharany, M. K., & El-Said, E. M. S. (2022), A Comparative Numerical Study of Shell and Multi-Tube Heat Exchanger Performance with Different Baffles Configurations. *International Journal of Thermal Sciences*, vol. 179, p. 107655.

Mehrjardi, S. A. A., Khademi, A., and Safavi, S. M. M. (2024), Performance Increasement in Shell-and-Tube Heat Exchangers Reinforced with Dimpled Tubes: A Correlation-Based Approach. *Int. J. Heat Mass Transf.*, vol. 226, p. 125489.

Mohammadzadeh, A. M., Jafari, B., and Hosseinzadeh, K. (2024), Comprehensive Numerical Investigation of the Effect of Various Baffle Design and Baffle Spacing on a Shell and Tube Heat Exchanger, *Appl. Therm. Eng.*, vol. 249, p. 123305

Bougriou, C., and Baadache, K. (2010), Shell-and-Double Concentric-Tube Heat Exchangers, *Heat Mass Transf*. vol. 46(3), pp. 315–322.

Ozden, E., and Tari, I. (2010), Shell Side CFD Analysis of a Small Shell-and-Tube Heat Exchanger, *Energy Convers. Manag*., vol.51(5), pp. 1004–1014.

Yang, J.-F., Zeng, M., and Wang, Q.-W. (2015), Numerical Investigation on Shell-Side Performances of Combined Parallel and Serial Two Shell-Pass Shell-and-Tube Heat Exchangers with Continuous Helical Baffles, *Appl. Energy*, vol.139, pp. 163–174.